$f_{7/2}$ proton alignment in ^{49}Cr

A. A. Pakou
Department of Physics, The University of Ioannina, GR-451 10 Ioannina, Greece
and Department of Physics, The University of Manchester, Manchester, United Kingdom

J. Billowes, A. W. Mountford, and C. Tenreiro*
Department of Physics, The University of Manchester, Manchester, United Kingdom

D. D. Warner
Daresbury Laboratory, Warrington, United Kingdom
(Received 10 March 1993)

The magnetic moment and lifetime of the $19/2^-$, 4.367 MeV state in ^{49}Cr have been measured in a transient magnetic field experiment. The nuclei were excited in the ^{12}C(^{40}Ca,2pn)^{49}Cr reaction and recoiled in a thick polarized gadolinium foil. The field strength was calibrated by a simultaneous g-factor measurement of excited states in ^{50}Cr and ^{46}Ti. The mean lieftime, found from Doppler-shifted line-shape analysis, is $\tau(19/2^-)=2.7(2)$ ps and the g factor is $g=+0.78(12)$. The g value implies a substantial $f_{7/2}$ proton contribution to the total spin of this state and the result is discussed in terms of both the shell model and the cranked shell model.

PACS number(s): 27.40.+z, 21.10.Ky, 21.60.Cs, 21.60.Ev

I. INTRODUCTION

In a recent paper on the spectroscopy of high spin states in ^{49}Cr by Cameron *et al.* [1], a discontinuity was reported at the $17/2^-$ state, which they suggested could be interpreted in terms of quasiparticle alignment within the framework of the cranked shell model. This description was supported by a dramatic increase in the Coulumb energy difference, $E_x(^{49}\mathrm{Mn})-E_x(^{49}\mathrm{Cr})$, which is understood by recalling that (using the familiar blocking arguments) the alignment in ^{49}Cr must involve two protons, while the alignment in ^{49}Mn involves two neutrons. This phenomenon is of particular interest because it may provide an important bridge, linking pure shell-model methods to the macroscopic methods of collective nuclear motion. The ^{49}Cr nucleus seems to exhibit some properties expected of a cranked deformed potential but lies in a region that may be reasonably described by the shell model.

We have extended the experimental study of this apparent alignment by measuring the lifetime and g factor (by the transient field method) of the first $19/2^-$ state at 4.367 MeV which lies immediately above the crossing region. This state was known to have a lifetime longer than a picosecond and thus suitable for a transient magnetic-field determination of its magnetic moment. The method has been described in detail by Benczer-Koller *et al.* [2] and we outline below features of this particular work. The method involves detecting the quite small precession ($\sim 1°$) acquired by a nucleus, when recoiling through a ferromagnetic medium, by measuring the rotation of the decay γ-ray angular distribution pattern. The rotation, $\Delta\theta$, is then directly proportional to the nuclear g factor and the time-integrated transient field strength:

$$\Delta\theta=-\frac{g\mu_N}{\hbar}\int_0^{t_s}B_{TF}(v,Z)e^{-t/\tau}dt \quad (1)$$

where τ is the mean lifetime of the nuclear state and t_s is the stopping time of the nucleus in the ferromagnetic and is typically about 1 ps. To produce the largest possible precession, the $19/2^-$ state was excited in an inverted heavy-ion reaction, giving a high initial recoil velocity and consequently a long t_s. In order to obtain the highest time-integrated field strength, gadolinium was used as the ferromagnetic host, despite the additional problems associated with its magnetization. The field strength was calibrated simultaneously with the ^{49}Cr measurement through a comparison of precessions of nuclear states in ^{50}Cr and ^{46}Ti with known moments and excited by the same heavy-ion reaction. The side-feeding times and lifetimes of states in the cascade were determined from the experimental data by a line-shape analysis of the Doppler-shifted γ-ray data.

II. EXPERIMENTAL DETAILS AND ANALYSIS

States in ^{49}Cr were populated in the ^{12}C (^{40}Ca,2pn) reaction at a beam energy of 140 MeV. The 500 μg/cm^2 carbon target layer was deposited on the surface of a thick gadolinium foil from a graphite-suspension spray. The reaction products recoiled with high initial velocity into the gadolinium foil which was backed by a copper foil serving as a thermal dissipator and was itself thermally linked to a liquid nitrogen trap. The gadolinium foil was prepared by rolling and then annealing in vacuum at 600 °C. Its magnetization was measured as a function of

*On leave from Department of Physics, University of São Paulo, Caixa Postale 20516-01498, Brazil.

field and temperature in a low-temperature magnetometer and was found to be 80% magnetized in the field of 0.12 T used in this experiment. The tandem beam current was limited to 5 nA to avoid further reduction through local beam heating. The gadolinium foil was polarized in the field of an electromagnet that was periodically reversed every 100 s. As the excited nuclei recoiled in the gadolinium they precessed in the transient magnetic field. This precession results in a rotation of the initial muclear alignment plane created by the reaction. The rotation was deduced from the change in the decay γ-ray distributions, as the direction of the polarizing field was periodically reversed. The γ-rays yields were monitored by four Compton-suppressed Ge detectors at $\pm 60°$ and $\pm 120°$ with respect to the beam axis, where the rate of change of the γ-ray intensity with angle is close to a maximum. Eight NE213 neutron detectors were also included in the setup and both singles and neutron-gated spectra were collected. A partial γ ray, Compton-suppressed spectrum is shown in Fig. 1.

Measurements of the logarithmic slopes, $S(\theta) = (1/W)(dW/d\theta)$, of the γ-ray distributions were carried out during the course of the experiment by moving the detectors by 4° either side of their original position to imitate a known rotation of the distributions. In addition, an angular distribution measurement was performed to corroborate the slope measurements. This was carried out with four detectors fixed at 15°, 75°, 105°, and −45°. The relative efficiency of these angle sets was measured with a ^{152}Eu source at the target position.

A. The transient field rotations

Nuclear precession angles $\Delta\theta$ were deduced from the counting ratios of adjacent pairs of detectors for the two field directions:

$$\rho_{1,2} = \frac{N_1(\uparrow)}{N_1(\downarrow)} \frac{N_2(\downarrow)}{N_2(\uparrow)}, \quad \rho = \sqrt{\rho_{1,2}\rho_{3,4}} \tag{2}$$

where $N_1(\uparrow)$ refers to the counts in a γ-ray peak in the spectrum of detector 1 with external polarizing field up. The counts contained in the Doppler-shifted tail were excluded from the analysis. The rotation is then given by

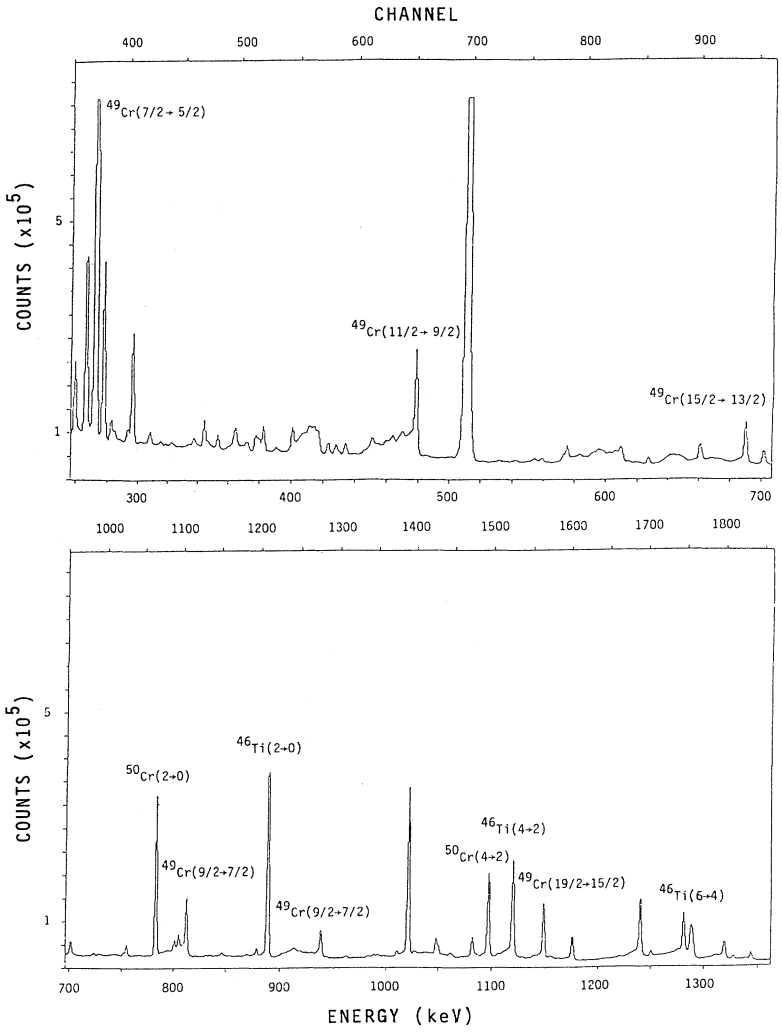

FIG. 1. Partial Compton-suppressed γ-ray spectrum. The detector was set at 116°.

TABLE I. g factors, precessions, and angular distribution logarithmic slopes $S(\theta)=(1/W)(dW/d\theta)$ observed in the present experiment.

	$J_i^\pi \rightarrow J_f^\pi$	τ^e (ps)	E_γ (keV)	$(v/v_0)^a_{in}$	$S(60°)$	$\Delta\theta$ (mrad)	g factor
^{49}Cr	$19/2^- \rightarrow 15/2^-$	2.7(2)	1177	7.8	−0.62(6)	−79.0(90)	+0.78(12)
	$7/2^- \rightarrow 5/2^-$	18.8(43)	272		+0.46(1)	−35.4(14)[b]	+0.35(7)[c]
^{50}Cr	$2^+ \rightarrow 0^+$	12.1(12)	783	7.8	−0.68(3)	−57.6(31)	+0.55(10)[d]
	$4^+ \rightarrow 2^+$	3.2(4)	1098		−0.69(4)	−51.4(40)	
	$6^+ \rightarrow 4^+$	1.8(4)	1283		−0.67(6)	−57.4(61)	
	$8^+ \rightarrow 6^+$	<4	1581		−0.67(7)	−57.5(98)	
^{46}Ti	$2^+ \rightarrow 0^+$	6.5(7)	886	8.0	−0.46(3)	−46.0(4)	+0.48(8)[d]
	$4^+ \rightarrow 2^+$	2.6(3)	1121		−0.47(5)	−53(7)	

[a]Recoil velocity on entry into the gadolinium foil in units of the Bohr velocity $v_0=c/137$.
[b]Rotation corrected for discrete feeding contributions.
[c]Effective g factor.
[d]Mean of published values taken from Ref. [6].
[e]Present data and Refs. [12,22].

$$\Delta\theta=\frac{1}{S(\theta)}\frac{\sqrt{\rho}-1}{\sqrt{\rho}+1}\ . \tag{3}$$

Since the counts contained in the Doppler-shifted tail were excluded in the analysis, the term $e^{-t/\tau}$ is omitted from Eq. (1), which corrects for the decays in flight. The experimental values of $\Delta\theta$ are shown in Table I, together with other details of the measurement.

The side-feeding times, which are discussed in Sec. II C, were found to be very fast (less than 100 fs) and so these decays were occurring predominantly in the carbon target layer and thus before the transient field begins to act. Such short feeding times were expected for our relatively low beam energy and have been reported before in this mass region [3,4] and also in the mass-80 region [5]. The discrete feeding is slower and must be considered separately.

The $19/2^-$ state is fed partially by the second $19/2^-$ (5.965 MeV) level, which is itself fed from the $23/2^-$ (8.009 MeV) level. The effective lifetime of the second $19/2^-$ level determined in the present experiment is 0.20(2) ps and was considered too short to significantly affect the rotation of the first $19/2^-$ state.

The yrast $7/2^-$ state is intriguing since only 37% of its population is due to feeding from the known discrete states, so 63% appears to be direct. We were not able to measure the speed of this particular feeding since the $7/2^-$ lifetime is too long to allow analysis of its Doppler-shifted tail. We were able to measure its transient field rotation and we can thus quote an "effective" g factor for this level once a correction is made for the rotation inherited mainly from the $19/2^-$ state through the yrast cascade as

$$\Delta\theta_{7/2}=\Delta\theta^{\rm meas}_{7/2}+\frac{a}{1-a}\frac{S(19/2\rightarrow\ldots 7/2\rightarrow 5/2)}{S^{\rm dir}(7/2\rightarrow 5/2)}\times(\Delta\theta^{\rm meas}_{7/2}-\Delta\theta^{\rm meas}_{19/2}) \tag{4}$$

where a represents the percentage of feeding from the known discrete states, $S(19/2\rightarrow\ldots 7/2\rightarrow 5/2)$ is the slope of the unobserved $7/2\rightarrow 5/2$ transition due to the $19/2$ cascade and $S^{\rm dir}(7/2\rightarrow 5/2)$ is the slope of the $7/2\rightarrow 5/2$ distribution, if the state was directly excited. Application of the above relation amounted to an 8% correction of the measured rotation.

However, we cannot determine whether the $7/2^-$ rotation was acquired in the (unobserved) feeding states or in the $7/2^-$ state itself. We will return to this point in the discussion.

B. The transient field calibration

There is a considerable variation in the magnetic properties of gadolinium foils which presumably depends on precise details of their preparation. Thus using a field parametrization, as is frequently done in the case of iron foils, would be unreliable here and not solely due to the rather sparse published information available. Fortuitously, the chosen reaction for ^{49}Cr also populated yrast states in ^{50}Cr and ^{46}Ti. These are moderately collective nuclei: the $B(E2;2^+\rightarrow 0^+)$ is 19 W.u. for both and the mean of published g-factors [6] for their 2^+ states are +0.55(8) and +0.48(8), respectively. Within the errors, the observed transient field rotations are constant in the ^{50}Cr yrast band up to the 8^+ state while the two observed precession for the 4^+ and 2^+ states in ^{46}Ti are also similar. These are thus behaving like collective nuclei which would then have g factors close to the collective value $g\approx Z/A$ ($Z/A=+0.480, +0.478$, respectively) for all yrast states. We have taken a weighted mean of the yrast band rotations as representative of the collective rotation and quote the ^{49}Cr g factors by comparison with the ^{50}Cr and ^{46}Ti rotations. The static field for Cr in Gd is known to be very small [7] and has not been considered. Full details of the g factor results are shown in Table I. If the field strength deduced for the present experiment is compared with the Chalk River parametrization [8]

$$B_{TF}=M154.7Z(v/v_0)\exp(-0.135v/v_0) \tag{5}$$

then the experimental field appears to be enhanced by a

factor of 1.3 using our value of $M=1720$ T, obtained from the magnetometer measurement. Such enhancements have been reported recently for ^{36}Ar and ^{41}Ca recoiling in thin Gd foils [4].

C. Lifetimes and side-feeding times

The neutron-gated spectra were used for the line-shape analysis and effective lifetimes of a number of levels in ^{49}Cr were obtained. By "effective" here we mean the lifetime obtained from the line shape assuming the side-feeding was instantaneous, while correctly accounting for the discrete feeding in the experimentally determined cascade. The side-feeding intensity is the difference between the total intensity of transitions out of a particular state and the total of all observed discrete transitions into that state. The side-feeding intensities, determined through the angular correlation measurement (A_0 values), are shown in the experimental spectrum of Fig. 2, as a percentage of the $7/2^- \rightarrow 5/2^-$ (272 keV) γ-ray total measured intensity. Forward and backward angle spectra ($+60°$ and $+120°$, for example) were compared and background lines which affected one angle but not the other angle could be subtracted. The best-fit lifetimes were obtained through a χ^2 analysis of the Doppler-shifted lineshapes assuming zero side-feeding times using the computer code GNOMON [9] and the electronic stopping powers of Ziegler, Biersack, and Littmark [10] (although similar results were obtained using stopping powers of the Lindhard-Scharff-Schiott theory [11]). Examples of the best fits for two of the states are shown in Fig. 3, and the results are compared with published measurements [12] in Fig. 2. Quoted errors are mainly due to uncertainties in the stopping powers as the statistical error was very small. The fits could not be significantly improved by introducing a nonzero side feeding time and we considered an upper limit on the side-feeding time to be <100 fs.

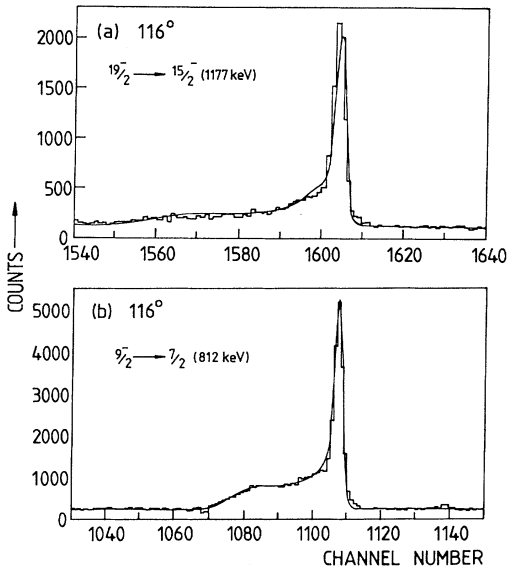

FIG. 3. Examples of line-shape fits to (a) the 1177 keV transition from the $19/2^-$ state observed at 116° and (b) the 812 keV transition from the $9/2^-$ state observed at the same angle.

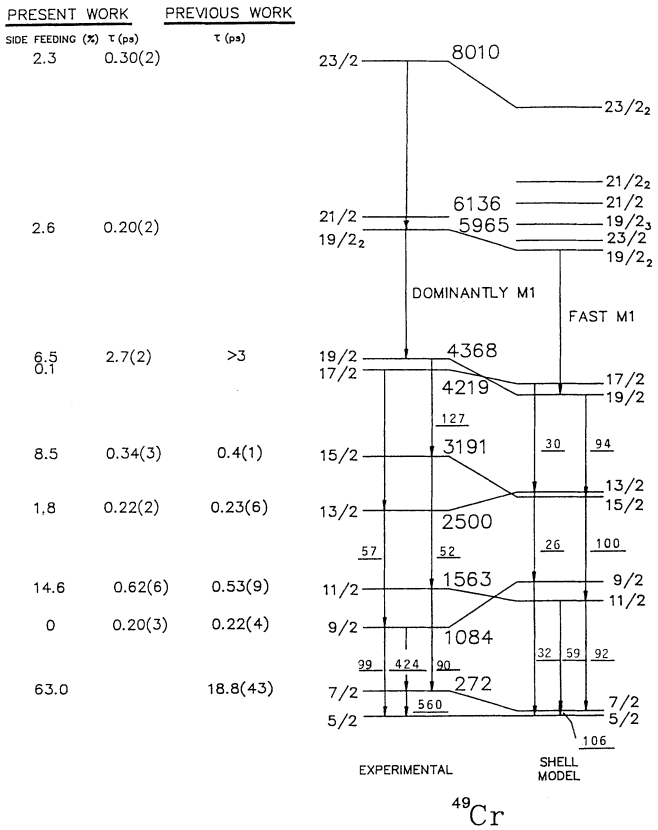

FIG. 2. A comparison of the experimental level scheme for the negative-parity states of ^{49}Cr (Ref. [1]) with the results of the shell-model calculation in the $f_{7/2}$ shell. The underlined numbers are $E2$ transition strengths in $e^2\,\mathrm{fm}^4$. The lifetime results from the line-shape analysis of the present work are also compared with previous values in the 2nd and 3rd columns.

Comparing our effective lifetimes (Fig. 2) with those obtained via prompt reactions, it can be seen that there is very good agreement and no evidence here of any delay in population in the heavy-ion reaction due to any detectable side-feeding time.

III. DISCUSSION

The yrast level scheme of ^{49}Cr obtained from the γ-ray spectroscopy of Cameron *et al.* [1] is shown in Fig. 2. The $E2$ transition strengths (in units of $e^2\,\mathrm{fm}^4$) shown in the figure have been deduced from the measured lifetimes and published mixing ratios and conversion coefficients [12,13]. These are compared with the $(f_{7/2})^9$ shell-model calculation using the computer code OXBASH [14] with the interaction of Kutschera *et al.* [15] derived from the ^{42}Sc spectrum. The $E2$ transition strengths have been calculated using effective charges of $1.5e$ for the proton and $0.5e$ for the neutron. The striking difference between the two level schemes has been discussed in some detail by Cameron *et al.* [16] and they attribute the apparent

failure of the shell model to the restricted basis employed; the experimental excitation energies of the first six states follow more closely the $J(J+1)$ dependence expected for a rigid rotor and this collective motion is reflected in the large $B(E2)$ strengths for the $\Delta I=1$ transitions between the low spin states which are not reproduced by the shell model. On the other hand, the $\Delta I=1$ transition mixing ratios, although poorly known, become rapidly smaller above the $9/2^-$ state, signifying weaker $B(E2)$ strengths. None of the $\Delta I=2$ $E2$'s, are particularly strong and the shell model is in reasonable accord with experiment for these decays. The $E2$ strength for the $19/2^-\rightarrow 15/2^-$ transition deduced from the lifetime measured in the present work is comparable to all the lower $\Delta I=2$ transition strengths and is also well reproduced by the shell-model calculation. Moreover as it is seen in Fig. 2, the higher levels that feed into the $19/2^-$ state, on the basis of excitation energies and decay characteristics, are well reproduced by the calculation.

Summarizing, above the $15/2^-$ state the shell model seems to provide an adequate description. On the other hand, the collective rotational behavior of ^{49}Cr is a prerequisite for describing the backbend at the $17/2^-$ level as a rotational alignment of two $f_{7/2}$ protons, as suggested by Cameron *et al.* [16] and Sheikh *et al.* [17]. Then, the justification for using the cranked shell model concerns the level spacing before the anomaly and the big $B(E2)$'s for the very low levels. The collectivity for higher levels in terms of reduced decay probabilities is weakened, but may have some validity even when the $E2$ enhancements are only 10 W.u.

We turn now to the g factors and in particular the result $g(19/2^-)=+0.78(12)$ that was found in the present work. In the rigid rotor model we would naively expect the higher spin-state g factors to asymptotically approach g_R. For odd-neutron nuclei g_R is systematically less than Z/A by about 0.1 (at least in the rare-earth region) and since the experimental moment is about twice this value, this indicates that the protons must be contributing substantially more to the total spin than the neutrons. It is interesting to compare the g factor predictions of the shell model and cranked shell model for the entire yrast band and this is shown in Fig. 4. In both sets of calculations the intrinsic spin has been scaled by the usual normalization factor of $g_s=0.7g_s$ (free). We have used the $(f_{7/2})^9$ wave functions described above for the shell-model calculation. The model actually predicts a monotonic increase in g with excitation energy, but this appears staggered in Fig. 4 when plotted against increasing spin.

The Routhian plots shown in Fig. 5 were generated from a cranked shell-model calculation [18] using 16 protons between shells $N=3$ to 4. The quadrupole deformation of $\varepsilon_2=0.18$ was deduced from the $7/2^-$ lifetime assuming a rigid rotor model, with $\gamma=0$ (the results are not sensitive to γ deformation). The hexadecapole deformation was taken to be zero since it was found that small negative or positive values did not appreciably change the results. The κ,μ values were taken from Ref. [19] and the proton pairing interaction $\Delta/\hbar\omega_0=0.088$ was calculated according to Ref. [20]. The results show a crossing frequency at 0.57 MeV/$\hbar$ and a gain in alignment of 4.7$\hbar$ through the crossing—close to the maximum of 6$\hbar$ expected for an $f_{7/2}$ proton pair alignment. From this model we have estimated the aligned proton angular momentum i_2 for each yrast state and then calculated the g factors using the formula [21]

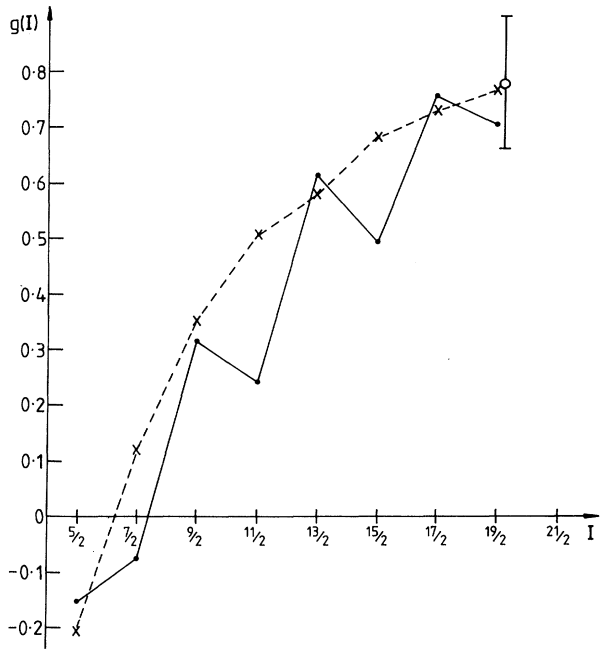

FIG. 4. A graphical comparison of yrast state g factors predicted by the $f_{7/2}$ shell model (full line) and the cranked shell model (dashed line). The one data point is the result of the present work. The ground-state g factor is known to be $g(5/2)=0.190(1)$ but its sign is undetermined.

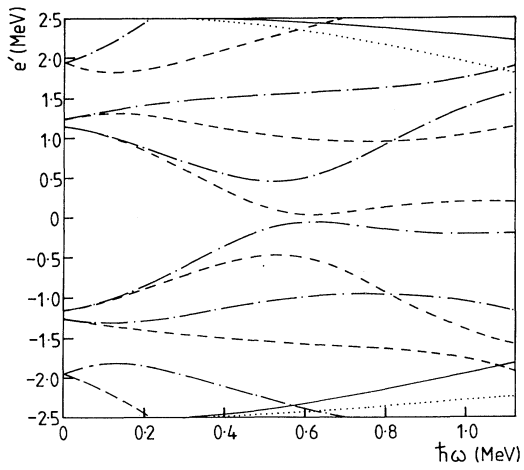

FIG. 5. Results of the cranked shell model described in the text for proton quasiparticle energies in the rotating frame vs frequency. The parameters used were $N=16$, $\varepsilon_2=0.18$, $\varepsilon_4=0$, $\Delta/\hbar\omega_0=0.088$. The parity-signature assignments are $++1/2$ (solid line), $+-1/2$ (dotted line), $-+1/2$ (dot-dashed line), and $--1/2$ (dashed line).

$$g(I)=g_R+(g_1-g_R)f_1+(g_2-g_R)f_2 \quad (6)$$

where the subscripts 1 and 2 refer to the deformation-aligned $f_{7/2}$ neutron and the rotationally aligned $f_{7/2}$ protons, respectively. The geometrical factors are

$$f_1=\{K^2+i_1[I(I+1)-K^2]^{1/2}\}/I(I+1)\ , \quad (7)$$

$$f_2=i_2[I(I+1)-K^2]^{1/2}/I(I+1)\ , \quad (8)$$

while g_1 and g_2 are the Schmidt values

$$g_i=g_j=g_l+(g_s-g_l)(2l+1)^{-1} \quad (9)$$

after scaling the intrinsic spin moment by a factor of 0.7 to account for core polarization and pion-exchange effects.

We have assumed $K=5/2$ and used a somewhat arbitrary aligned contribution of $i_1=1/2$ for the neutron (the general trend of the results is not very sensitive to this parameter). The proton alignment i_2 reaches a (calculated) value of 4.2 in the $19/2^-$ state. The variation of g factor with spin is readily understood; initially there is a rapid rise from the intrinsic value towards $g_R(=+0.49$ here) and then the extra contribution from the proton alignment develops above the $13/2^-$ state. What is remarkable is the similarity of the predictions of the two models. Moreover, both satisfactorily reproduce the experimental $g(19/2^-)$ value. The magnitude of the ground-state g factor is known [6], $g=0.190(1)$ but the sign is undetermined. If it were negative (as it is for every other odd-neutron nucleus in the $f_{7/2}$ shell) it would be in good agreement with both calculations. The difficulty lies then in explaining the effective g factor of $+0.35(5)$ for the $7/2^-$ state; if this truly reflects the 7/2 g factor itself (there is not sufficient information on its feeding history to establish this) then it cannot be explained by either model. However, we might speculate that in this localized region of collectivity the ground-state moment is positive, in which case we would deduce from Eq. (6) an effective factor g_1, of $g_1=+0.12$ and subsequently the g-factor of the 7/2 state as $g(7/2^-)=+0.31$. The cranking model predictions for the higher spins are not greatly affected by the value of g_1, but a positive moment for the ground state would again highlight the deficiency of the $f_{7/2}$ basis in the shell model.

In conclusion, we have measured the lifetime and magnetic moment of the first $19/2^-$ state in ^{49}Cr. An adequate explanation of the dominant proton contribution implied by the large g factor can be provided by both the shell model (which fails in its description of the lower-spin states) and the cranked shell model, which seems less applicable here because of the low collectivity. Nevertheless, two very different models have produced strikingly similar descriptions of the magnetic moment characteristics. Shell-model calculations in an extended basis would be of great interest in this region to further explore the bridge between microscopic and macroscopic descriptions.

ACKNOWLEDGMENTS

We would like to thank Dr. P. W. Mitchell for valuable discussions concerning the magnetic properties of the gadolinium backing in our target and Dr. P. W. Mitchell and D. Dyke for their help in running the gadolinium magnetization measurements.

[1] J. A. Cameron, M. A. Bentley, A. M. Bruce, R. A. Cunningham, W. Gelletly, H. G. Price, J. Simpson, D. D. Warner, and A. N. James, Phys. Lett. B **235**, 239 (1990).
[2] N. Benczer-Koller, M. Hass, and J. Sak, Annu. Rev. Nucl. Part. Sci. **30**, 53 (1980).
[3] H. P. Hellmeister, K. P. Lieb, and W. Muller, Nucl. Phys. **A307**, 515 (1978).
[4] A. A. Pakou, F. Brandolini, D. Bazzacco, P. Pavan, C. Rossi-Alvarez, E. Maglione, M. DePoli, and R. Ribas, Phys. Rev. C **45**, 166 (1992).
[5] A. W. Mountford, J. Billowes, W. Gelletly, H. G. Price, and D. D. Warner, Phys. Lett. B **279**, 228 (1992).
[6] P. Raghavan, At. Data Nucl. Data Tables **42**, 189 (1989).
[7] W. D. Brewer and E. Wehmeier, Phys. Rev. B **12**, 4608 (1975).
[8] O. Häusser, H. R. Andrews, D. Horn, M. A. Love, P. Taras, P. Skensved, R. M. Diamond, M. A. Deleplanque, E. D. Dines, A. O. Machiavelli, and F. S. Stephens, Nucl. Phys. **A412**, 141 (1984).
[9] H. P. Hellmeister and L. Lumann, computer code GNOMON (Göttingen, 1983) (unpublished).
[10] J. F. Ziegler, *The Stopping and Range of Ions in Matter* (Pergamon, New York, 1985).
[11] J. Lindhard, M. Scharff, and H. E. Schiott, Mat. Fys. Medd. **33**, 14 (1963).
[12] T. W. Burrows, Nucl. Data Sheets **48**, 569 (1986).
[13] P. Möller and J. R. Nix, At. Data Nucl. Data Sheets **26**, 165 (1981).
[14] B. A. Brown, A. E. Etchegongen, W. D. M. Rae, and N. S. Goodwin, OXBASH—The Oxford-Buenos-Aires-MSU Shell Model code, Michigan State University Cyclotron Laboratory International Report No. MSUCL-521, 1986 (unpublished).
[15] W. Kutschera, B. A. Brown, and K. Ogawa, Riv. Nuovo. Cimento **1**, 12 (1978).
[16] J. A. Cameron, M. A. Bentley, A. M. Bruce, R. A. Cunningham, W. Gelletly, H. G. Price, J. Simpson, D. D. Warner, and A. N. James, Phys. Rev. C **44**, 1882 (1991).
[17] J. A. Sheikh, P. Van Isacker, D. D. Warner, and J. A. Cameron, Phys. Lett. B **252**, 314 (1990).
[18] R. Bengtsson and S. Frauendorf, Nucl. Phys. **A327**, 139 (1979).
[19] S. G. Nilsson, C. F. Tsang, A. Sobiczewski, Z. Szymanski, S. Wyecech, C. Gustafsson, L. Lilam, P. Moller, and B. Nilsson, Nucl. Phys. **A131**, 1 (1969).
[20] R. Bengtsson, S. Frauendorf, and F. R. May, At. Data Nucl. Data Sheets **35**, 16 (1979).
[21] F. Donau and S. Frauendorf, in *Proceedings on High Angular Momentum Properties of Nuclei,* Oak Ridge, 1982, edited by N. R. Johnson (Harwood Academic, New York, 1983), p. 143.
[22] W. Dehnardt, O. C. Kistner, W. Kutschera, and H. J. Sann, Phys. Rev. C **7**, 1471 (1973).